Cloud Overlapping Detection Algorithm Using Solar and IR Wavelengths with GOES Data Over ARM/SGP Site

K. Kawamoto
Virginia Polytechnic Institute and State University
Blacksburg, Virginia

P. Minnis and W. L. Smith, Jr.
National Aeronautics and Space Administration
Langley Research Center
Hampton, Virginia

Introduction

One of the most perplexing problems in satellite cloud remote sensing is the overlapping of cloud layers. Although most techniques assume a one-layer cloud system in a given retrieval of cloud properties, many observations are affected by radiation from more than one cloud layer. As such, cloud overlap can cause errors in the retrieval of many properties including cloud height, optical depth, phase, and particle size. A variety of methods have been developed to identify overlapped clouds in a given satellite imager pixel. Baum et al. (1995) used CO_2 slicing and a spatial coherence method to demonstrate a possible analysis method for nighttime detection of multi-layered clouds. Jin and Rossow (1997) also used a multi-spectral CO_2 slicing technique for a global analysis of overlapped cloud amount. Lin et al. (1998) used a combination infrared (IR), visible (VIS), and microwave data to detect overlapped clouds over water. Recently, Baum and Spinhirne (2000) proposed a 1.6 and 11 μm bispectral threshold method. While all of these methods have made progress in solving this stubborn problem, none have yet proven satisfactory for continuous and consistent monitoring of multi-layer cloud systems. It is clear that detection of overlapping clouds from passive instruments such as satellite radiometers is in an immature stage of development and requires additional research. Overlapped cloud systems also affect the retrievals of cloud properties over the Atmospheric Radiation Measurement (ARM) domains (e.g., Minnis et al. 1998) and hence should be identified as accurately as possible. To reach this goal, it is necessary to determine which information can be exploited for detecting multi-layered clouds from operational meteorological satellite data used by ARM. This paper examines the potential information available in spectral data available on the Geostationary Operational Environmental Satellite (GOES) imager and the National Oceanic Atmospheric Administration (NOAA) Advanced Very High Resolution Radiometer (AVHRR) used over the ARM Program's Southern Great Plains (SGP), and North Slope of Alaska (NSA) sites to study the capability of detecting overlapping clouds.

Data

This study uses daytime half-hourly GOES-8 4-km data from channels 1, 2, 4, and 5, at VIS 0.65 μm, solar-IR 3.9 μm, IR 10.8 μm, and split-window (WS) 12.0 μm wavelengths, respectively, and the cloud

properties over the ARM SGP central facility (CF) derived from these radiances by Minnis et al. (2001) for all of 1998. The ARM 35-GHz radar data taken over the CF are used to provide cloud boundary data to determine the presence of single- and multi-layered clouds during each 10-minute period centered on a given GOES image time. The average GOES radiances and cloud properties for a 0.3° box centered on the CF are compared to the cloud boundary data from the corresponding radar data.

Methods and Results

Two methods for detecting multi-layered clouds are proposed. The first one relies on the brightness temperature difference between channels 4 and 5 (hereafter BTD_{45}). The basic assumption for this approach is that for large cloud optical depth τ, BTD_{45} should be small, nearly equal to zero, if the cloud is a single layer because the emissivities in both channels approach unity. On the other hand, if BTD_{45} is large and τ is large, a thin cloud probably overlaps a lower cloud. Thus, BTD_{45} should be an indicator of overlapping clouds when the τ is large. To illustrate this situation, Figure 1 shows the results of a numerical simulation using the parameterizations of Minnis et al. (1998). The values of BTD_{45} are plotted as functions of total optical depth (OD) and effective cloud particle size for single and 2-layer cases. The single cloud is ice layer with OD between 0.5 and 9.5 with an effective diameter D_e = 18, 30, 68, and 123 μm. The two-layer system consists of a low cloud τ = 10 and an effective droplet radius r_e = 10 μm overlaid by the high cloud used in the single-layer case. Cloud-top temperatures of 245 and 275 K are used for the high and low clouds, respectively. The figure demonstrates that the values of BTD_{45} for the two-layer cloud system are greater than their single-layered counterparts for a given value of total OD. In this case, values of BTD_{45} exceeding about 0.6K for $\tau > 8$ should indicate the presence of multi-layered clouds. Although a great variety of cloud temperature, OD, and particle size combinations will occur, BTD_{45} values should follow a pattern similar to that in Figures 1, 2, and 3 plot the observed BTD_{45} values as a function of the retrieved OD for both single- and multi-layered clouds having $BTD_{45} > 0.5$ K and $\tau > 10$ correspond to multi-layered clouds. For smaller BTDs, only 21 percent of the clouds are multi-layered. If a BTD_{45} of 1 K is used as the threshold, 85 percent of the clouds are multi-layered for larger BTD_{45}, but 28 percent of the multi-layered clouds would be identified as single-layered. At lower ODs, BTD_{45} is generally greater than that from the single-layer clouds, but no clear threshold values are evident for selecting single- versus multi-layered clouds.

For clouds identified as ice (Figure 3), only 60 percent of the pixels are clearly multi-layered using a threshold of BTD_{45} = 0.5 K for the optically thick clouds. Many of the optically thicker clouds have $BTD_{45} > 1.0$ K. If the threshold of 1.0 K is used for the ice clouds, 82 percent of the clouds with larger BTD_{45} are multi-layered and 36 percent of the clouds with smaller BTD_{45} are single layered. The differences between Figures 2 and 3 may be due to the low density of ice clouds and their IR scattering properties. Because the phase discrimination is based on models of cloud particle sizes, the ice cloud emissions probably dominate the clouds identified as ice, while those determined to be water most likely have only a thin layer of ice cloud over the low-level water cloud. The water clouds are generally dense so the radiating temperatures for both channels in the single-layer case are probably very close. Optically thin ice clouds can be several kilometers thick with vertically dependent microphysical properties. Optically thicker ice clouds also may be very thick physically with a layer of low-density cirrus at the top of the cloud. These low-density clouds or cloud layers could easily produce BTD_{45} = 1 K, even for optically thick clouds because of their vertical structure. Thus, detecting multi-layering

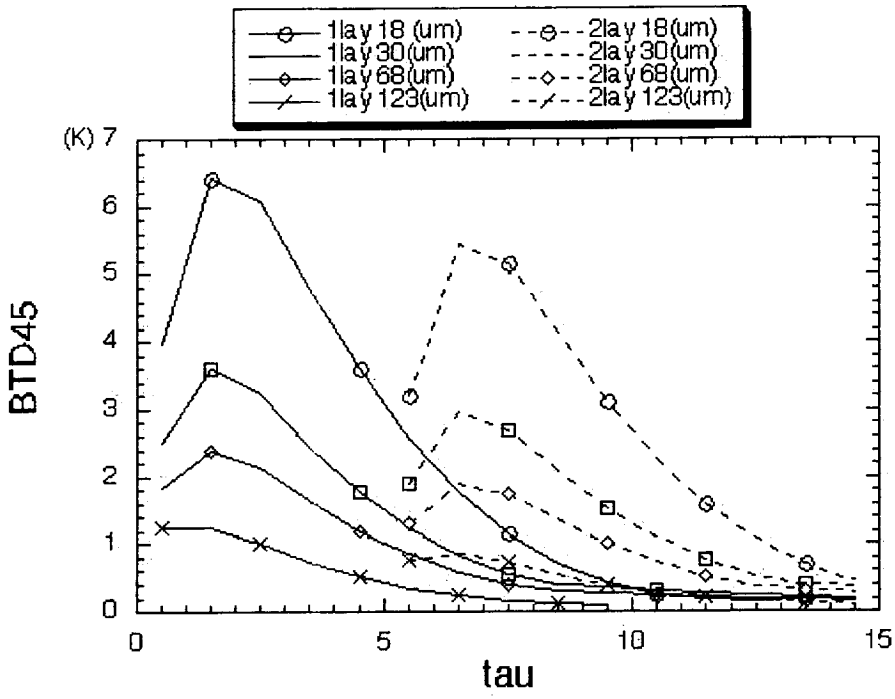

Figure 1. Theoretical brightness temperature differences for one- and two-layer cloud systems.

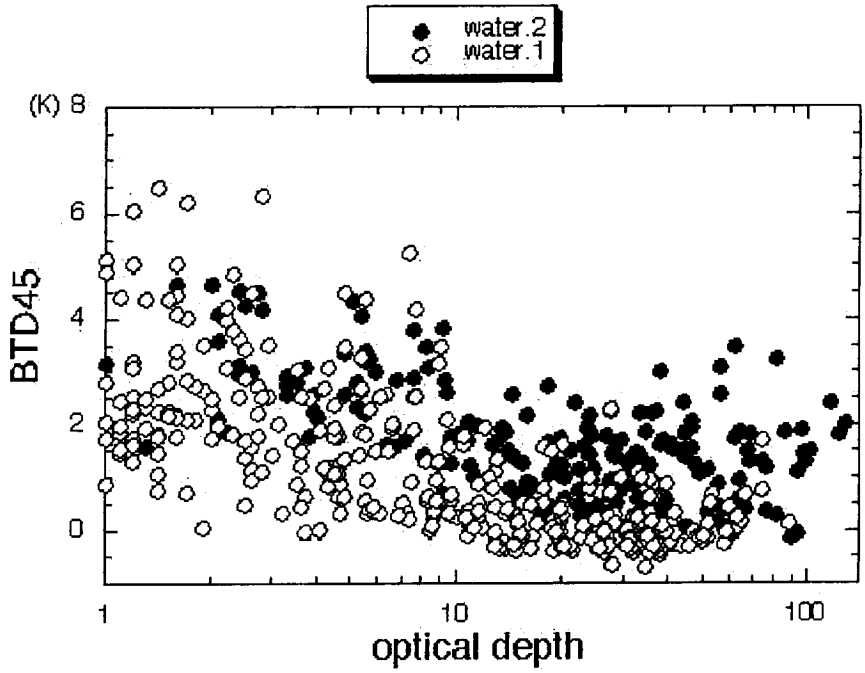

Figure 2. Brightness temperature differences for single- and multi-layered clouds over the CF identified as liquid phase only from GOES-8.

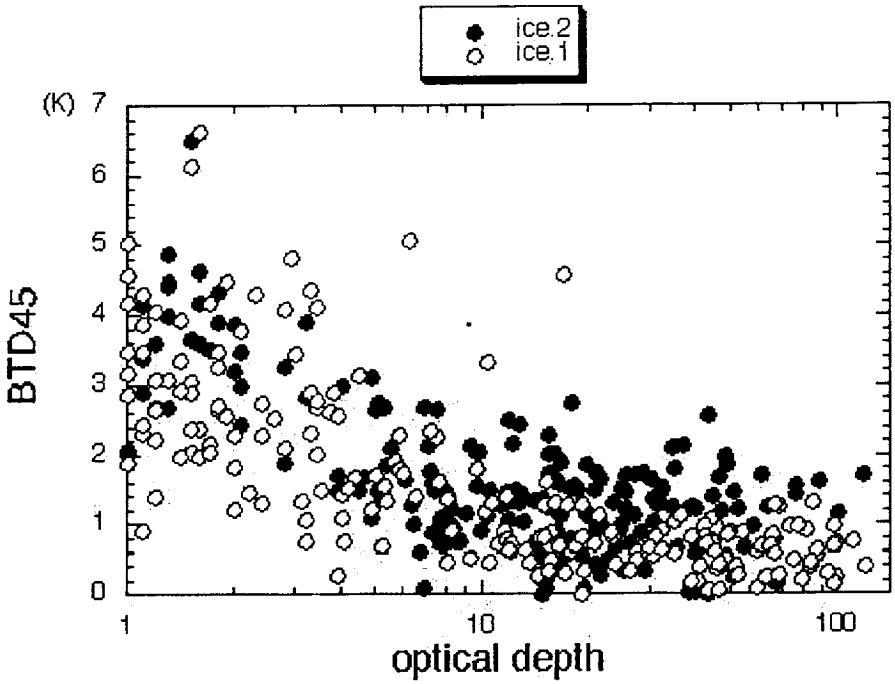

Figure 3. Same as Figure 2, except for clouds identified as ice phase only.

for clouds identified as ice is more difficult than for water clouds using this approach. The second method uses particle size for detecting overlapping clouds. The method applied by Minnis et al. (2001) assumes that the observed cloud in a given imager pixel is a single-layered cloud and uses the 3.7- and 11-μm brightness temperature difference between channels 3 and 4 (hereafter BTD_{34}) to determine phase and effective particle size. For a given value of τ, BTD_{34} is smallest for large ice crystals and greatest for small droplets. From the smallest water droplet radius, droplet size generally increases as BTD_{34} decreases. Conversely, starting with the largest ice crystal, effective diameter (D_e) decreases as BTD_{34} increases. The value of BTD_{34} may correspond to both large water droplets and small ice crystals for intermediate cases. Thus, if a relatively thin ice cloud overlaps a water cloud, the retrieved value of effective radius (r_e) or D_e may be either very large or extremely small, respectively, depending on the OD of the upper level cloud. Motivated by this idea, effective particle sizes were plotted against the retrieved OD values for single and multi-layered cases as determined by the 35-GHz cloud radar. Figures 4 and 5 show scatter plots for the water and ice cases, respectively. For larger ODs, very few single-layer clouds occur with $r_e > 15$ μm. However, some multi-layered clouds have smaller droplet radii. Both large and small droplet sizes occur for the smaller ODs with no clear distinction between the single- and multi-layered clouds. Pixels that are only partially cloud filled could be responsible for the larger values of r_e at small ODs. In the ice case, the multi-layer clouds generally correspond to $D_e <$ 70 μm for $\tau > 6$. At smaller ODs, large and small ice crystals occur for both single- and multi-layered systems. Histograms of the particle sizes for $\tau > 10$ are shown in Figures 6 and 7. As noted before, the largest droplets (Figure 6) correspond primarily to overlapped clouds, but many of the multi-layer systems yield values of r_e that are within the observed probability distribution for single-layer clouds. Better discrimination may be possible for the ice clouds because the single- and multi-layered D_e

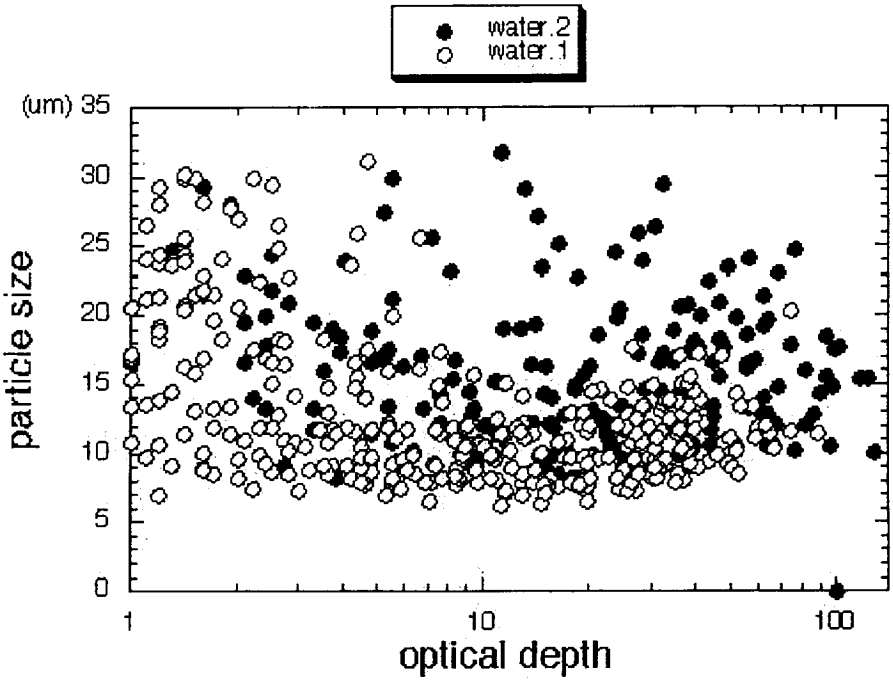

Figure 4. Effective droplet radius for single- and multi-layered liquid phase clouds from GOES-8.

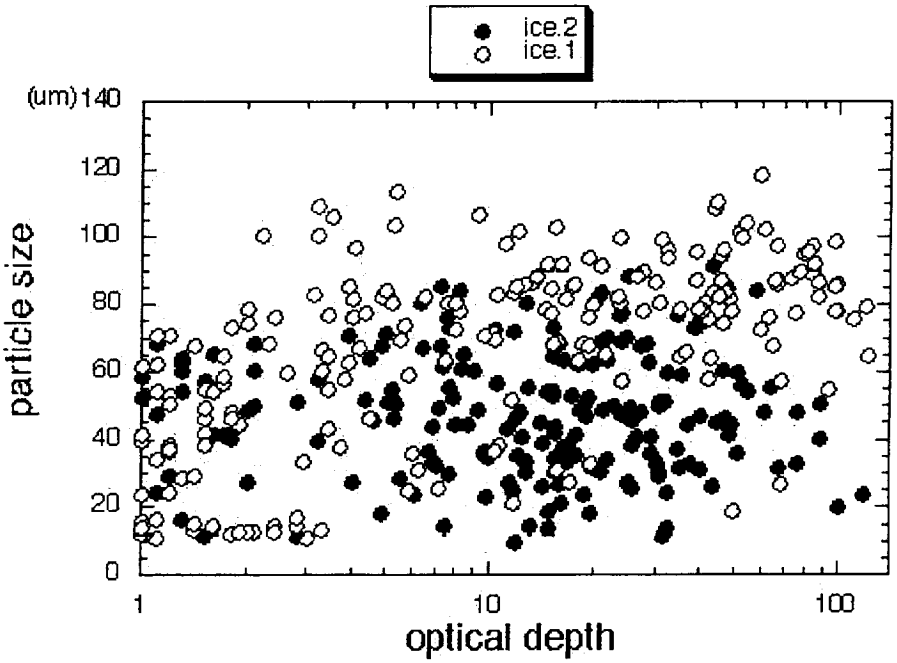

Figure 5. Same as Figure 4, except for ice phase only.

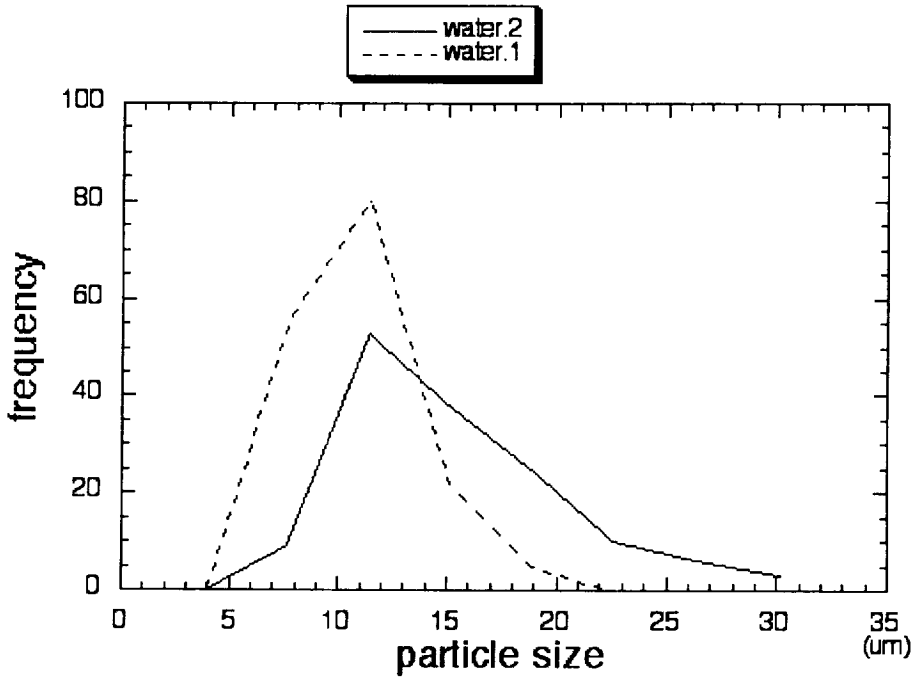

Figure 6. Histograms of cloud water droplet radius for single- and multi-layered clouds.

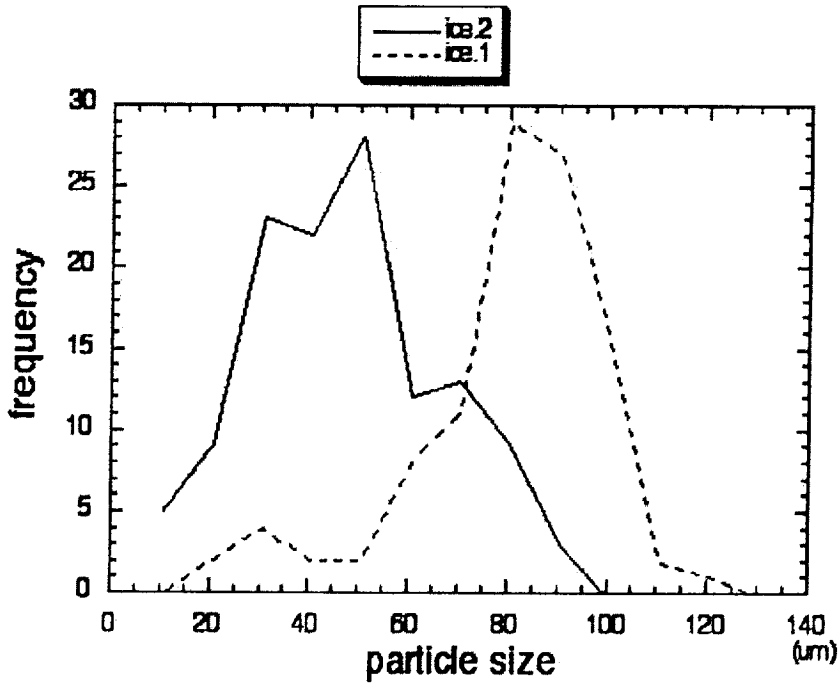

Figure 7. Same as Figure 6, except for cloud ice crystal diameter.

histograms are substantially different with peaks at 50 and 80 μm, respectively. Using a threshold of D_e = 70 μm would identify 84 percent of the multi-layered clouds having a total OD greater than 8. However, it would misidentify 23 percent of the single-layered clouds having relatively small ice particle sizes thus, skewing the ice crystal size distribution. By combining both methods, it may be possible to account for some of the weaknesses in the two techniques used alone. For example, the BTD_{45} data provide minimal discrimination for overlapped clouds identified as ice, but the particle size can be used to detect many of the overlapped ice clouds. Conversely, the particle size is not particularly helpful in the identification of many overlapped water clouds, but BTD_{45} appears to be useful in this case.

Discussion and Concluding Remarks

The results found here indicate that a multi-layered detection algorithm using BTD45 with the derived phase and particle sizes may provide accuracies of ~80 percent for cloud systems having optical depths greater than 8 to 10. Detection of multi-layered systems with smaller ODs or with better accuracy requires much additional study. The radar cloud multi-layering classification used a broad definition of cloud overlap. Precipitating clouds, broken clouds, and water-over-water and ice-over-ice clouds were included in the dataset. The amount of cloud layer separation was not specified, so that two layers only several hundred meters apart may have been included. By further subsetting the dataset using this additional information, it should be possible to refine the criteria needed to determine the presence of multi-level clouds. It will also be possible to define the conditions when this method is applicable.

This paper is the first step in developing a robust method for detecting multi-layered clouds using the satellite imager channels available for the most routine monitoring of clouds over the ARM sites. Further study will be devoted to examining the impact of cloud temperature, fraction, and layer gaps on the thresholds that could be used for identifying multi-layered clouds. By gathering similar datasets over the NSA and TWP sites, it should be possible to adjust any algorithm for the particular environment.

Acknowledgements

The authors are grateful to Seiji Kato for helping radar data processing and Robert Arduini for supplying radiative transfer calculation results.

Corresponding Author

K. Kawamoto, k.kawamoto@larc.nasa.gov, (757) 864-5673

References

Baum, B. A., J. M. Alvarez, T. Uttal, J. Intrieri, M. Poellot, E. Clothiaux, T. P. Ackerman, D. O'C. Starr, J. Titlow, and V. Tovinkere, 1995: Satellite remote sensing of multiple cloud layers. *J. Atmos. Sci.*, **52**, 4210–4230.

Baum, B. A., and J. D. Spinhirne, 2000: Remote sensing of cloud properties using MODIS airborne simulator imagery using SUCCESS, 3: Cloud overlap. *J. Geophys. Res.*, **105**, 11,793-11,801.

Jin, Y., and W. B. Rossow, 1997: Detection of cirrus overlapping low-level clouds. *J. Geophys. Res.*, **102**, 1727-1737.

Lin, B., P. Minnis, B. A. Wielicki, D. R. Doelling, R. Palikonda, D. F. Young, and T. Uttal, 1998: Estimation of water cloud properties from satellite microwave and optical measurements in oceanic environments. II: Results. *J. Geophys. Res.*, **103**, 3887-3905.

Minnis, P., D. P. Garber, D. F. Young, R. F. Arduini, and Y. Takano, 1998: Parameterizations of reflectance and effective emittance for satellite remote sensing of cloud properties. *J. Atmos. Sci.*, **55**, 3313–3339.

Minnis, P., W. L. Smith, Jr., and D. F. Young, 2001: Cloud macro- and microphysical properties derived from GOES over the ARM SGP domain. This proceedings.